Quantifying key parameters of environmental transmission and age-specific susceptibility for *Mycobacterium avium* subspecies *paratuberculosis (MAP)*

Yuqi Gao[1,2], Piter Bijma[2], Mart C.M. de Jong[1]

[1] Infectious Disease Epidemiology Group, Department of Animal Sciences, Wageningen University and Research, Wageningen, Netherlands

[2] Animal Breeding and Genomics Group, Department of Animal Sciences, Wageningen University and Research, Wageningen, Netherlands

* Corresponding author

E-mail: yuqi.gao@wur.nl (YG)

These authors contributed equally to this work.

Abstract

Paratuberculosis is a chronic disease in ruminants, caused by *Mycobacterium avium subspecies paratuberculosis* (*MAP*). This research aims to improve the understanding of transmission dynamics on both exposure and susceptibility—factors influenced by the shedders and the recipients, respectively. We present an age-specific dose-response model, where the decrease in recipient's susceptibility with age is quantified by a specific rate, and an environmental transmission model, where exposure from shedders is quantified by transmission rate parameters and the *MAP* decay rate in the environment. Parameters of both models were estimated based on published experiments. The age-specific susceptibility decrease rate was

calculated to be 0.0629 wk⁻¹. In the transmission model, two sub-models apply different standardization schemes for transiently infectious (Itr), low shedding (Il), high shedding (Ih): Model A standardized shedding rate at 2.29 wk⁻¹ and varied transmission rates across states ($\widehat{\beta_{Itr}}$: 0.0469 wk⁻¹, $\widehat{\beta_{Il}}$: 0.0272 wk⁻¹ and $\widehat{\beta_{Ih}}$: 0.329 wk⁻¹). Model B varied shedding rates across infectious states ($\widehat{sh_{Itr}}$: 2.29 wk⁻¹, $\widehat{sh_{Il}}$: 1.33 wk⁻¹, and $\widehat{sh_{Ih}}$: 16.1 wk⁻¹) while keeping the transmission rate constant at 0.0469 wk⁻¹. In both models, the *MAP* decay rate was estimated at 0.424 wk⁻¹. Then, a scenario study was done, focusing on understanding: changes in environmental contamination levels over time, the timing of exposure, the duration of exposure, and the recipient's age at exposure. Our findings enhance understanding of *MAP* transmission dynamics and support the development of future models that incorporate real-world complexities and interventions. The 95% confidence intervals for all estimates can be found in the main text.

Author Summary

Mycobacterium avium subspecies *paratuberculosis* (*MAP*) causes paratuberculosis (Johne's disease), a global concern in dairy farming that results in reduced milk production, health issues in cattle, and potential risk for food safety. In this study, we aimed to improve our understanding of MAP's environmental transmission dynamics, including its build-up, decay, and transmission (via environmental exposure). We explored how the timing, duration of exposure, and recipient age affect infection probabilities. Our analysis of previous experimental data revealed that susceptibility to infection decreases at a specific rate as animals age. We also assess how the decay of MAP and shedding from three types of infectious animals contributes to contamination. Our findings provide new insights into the transmission dynamics of

MAP and offer refined estimates of age-specific susceptibility decrease rate, three MAP shedding rates, three transmission rates and MAP natural decay rate. We hope this research can inform more effective control strategies, particularly those aimed at protecting younger animals and reducing environmental contamination.

Introduction

Paratuberculosis, caused by *Mycobacterium avium subspecies paratuberculosis* (*MAP*), is a chronic disease affecting ruminants (1). The disease is known for its long incubation period, inadequate diagnostic tests (especially for early stages), limited vaccination effect, and long survival in the environment, all of which alone or in combination could be the reason why *MAP* is difficult to control and eradicate(2-7). *MAP* can be transmitted horizontally via contaminated milk or faeces and vertically from dam to offspring (8, 9). A major obstacle in eradicating *MAP* is its environmental transmission, where contaminated environments can cause infections even in the absence of infectious individuals at that location and time.

Understanding environmental transmission is crucial for *MAP* dynamics; therefore, we applied an advanced mathematical model developed by Chang and De Jong (10) to study it. This model, which has proven effective for various diseases (10-13), was not yet used for *MAP*. The model incorporates three key parameters: shedding rate, decay rate, and transmission rate. Additionally, if spatial spread is considered, a fourth parameter, the diffusion rate, is necessary (12). For *MAP*, spatial transmission was simplified by considering three different environments on a dairy farm: the calving house, calf collective pen, and lactating cow stable. This research focuses on estimating the decay and transmission rate parameters, differentiated for individuals at various infectious states, following the approach of Chang and De Jong (10). The model assumes that once *MAP* is introduced into a clean environment, it is shed at a specific rate and exponentially decays over time based on its natural decay rate. The cumulative exposure is determined by integrating environmental contamination levels. Besides, this model accounts for transmission both with and without infectious

individuals present. For example, aerosol transmission can be modelled as rapid pathogen decay in airborne droplets, while milk transmission can be modelled as minimal decay with immediate exposure. This research aims to estimate all necessary transmission parameters to support the application of this model to *MAP*.

Accurate assessment of infection risk in *MAP* requires a thorough understanding of age-specific susceptibility. Newborns, probably because of their heightened intestinal permeability, are particularly vulnerable to *MAP* during the first 24 hours of life (14, 15). Susceptibility decreases with age, with cows generally considered susceptible only during their first year of life (16). However, infections in adult cows have been observed, but only when exposed to very high levels of *MAP*, such as through oral dosing of 3×10^{10} organisms or housing with 15 high shedders for 4 years (14, 17). The commonly used exponential model for age-specific susceptibility assumes a decrease rate of 0.1 wk^{-1} (16, 18-20). However, this rate is a broad estimate and could possibly be improved. This research addresses this gap by developing an age-specific dose-response model and estimating the susceptibility decrease rate parameter using data from fourteen inoculation experiments that include age at exposure. The study aims to more accurately capture how susceptibility to *MAP* varies with age and dose, and to enhance the precision of infection risk calculation.

This research will develop both an age-specific dose-response model and a stochastic environmental transmission model to estimate transmission rate parameters and their 95% confidence interval (95%CI) based on fourteen dose-response experiments and two transmission experiments. The parameters include susceptibility decrease rate (g), median infective dose (ID_{50}), transmission rate (β or

β_{state}), shedding rate (sh_{state} or sh), *MAP* decay rate in the environment (de), where $state$ is either transiently infectious (Itr), low shedding (Il) or high shedding (Ih). This classification of shedding patterns is consistent with the observed shedding patterns from transmission experiments. With the model we will then explore four scenarios: changes in contamination levels over time, timing and duration of exposure, and the recipient's age at exposure.

Results

Age-specific susceptibility decrease rate

The dose-response model was used to estimate infectious Dose 50 (ID_{50}) and age-specific decrease rate (g) values from *MAP* inoculation experiments in calves of different ages. The fit of non-linear model, based on an exponential distribution, results an ID_{50} estimate and its 95%CI of 2.75×10^6 (1.42×10^6, 4.08×10^6) CFU, and a g estimate and its 95%CI of 0.0629 (0.0446, 0.0811) wk^{-1}. The model's dose response curve (Fig. 1), which describes the probability of observing a new case in the inoculation experiments, is as follows:

$$p(dose, age) = 1 - e^{-\left(rS(age)\times\frac{\ln(2)}{2.75\times10^6}\right)\times dose}$$

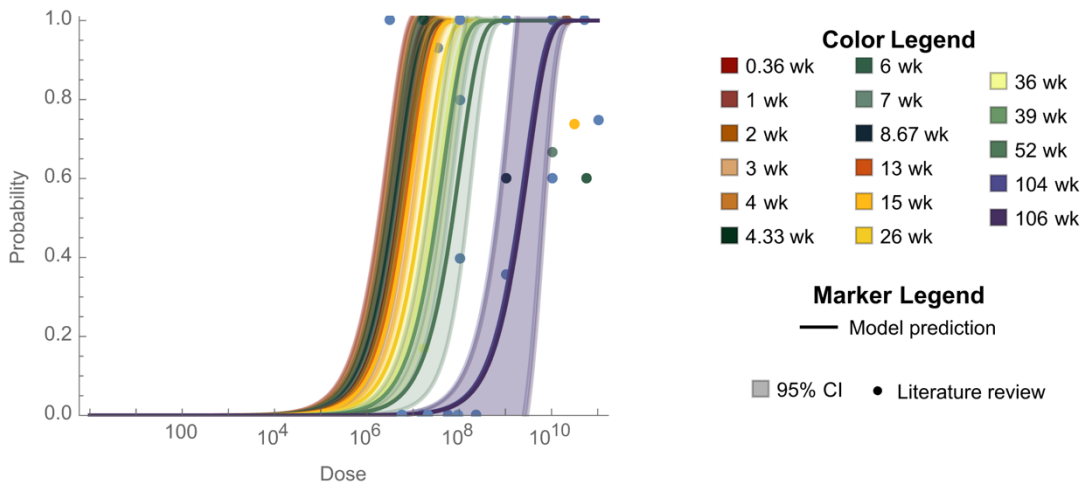

Fig 1. Dose-Response Curves Based on Experimental Data Sets. Experimental data, categorized by age, are represented by coloured dots. The predicted dose response curves for each age groups are shown as solid, coloured lines, with shaded areas representing the 95% confidence intervals.

Relatively susceptibility ($rS(age)$) decreases exponentially with age at a rate of 0.0629 wk⁻¹ and the average susceptibility ($\overline{rS}(age_i, age_i + \tau)$) within age range ($age_i, age_i + \tau$) is quantified by integrating the continuous $rS(age)$ function and diving it by the interval length. Equations are as follow:

$$rS(age) = e^{-0.0629 \times age}$$

$$\overline{rS}(age_i, age_i + \tau) = \frac{1}{\tau} \int_{age_i}^{age_i + \tau} e^{-0.0629 \times \alpha} d\alpha$$

As shown in Fig. 2, our model estimates a significant slower decrease rate in susceptibility with age compared to the previously published rate of 0.1. This suggests that infection probabilities for older cows have been underestimated.

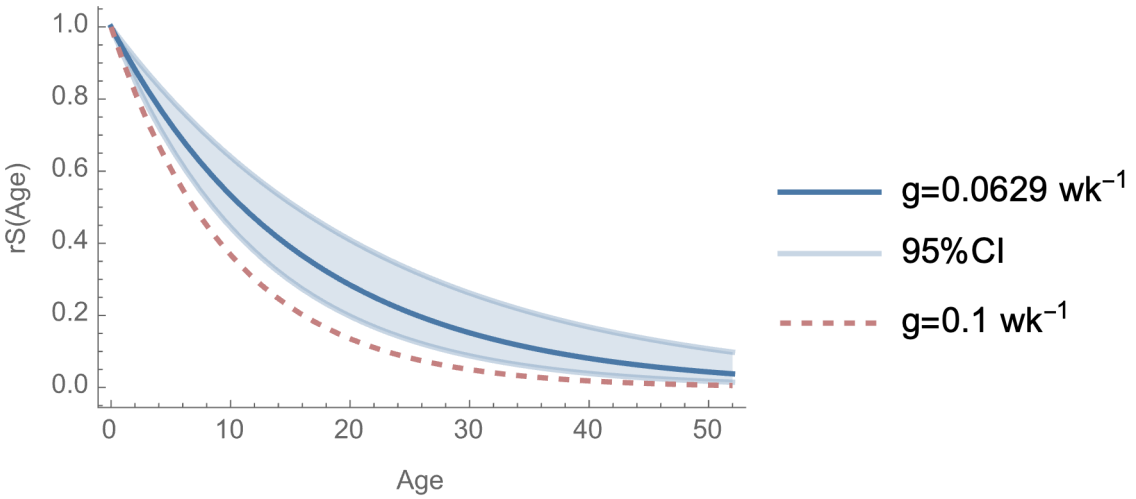

Fig. 2. Comparison of Susceptibility Decrease with Age. The solid line and shaded region represent the relative susceptibility decrease ($rS(age)$) with age based on our model-estimated rate (g = 0.0629) and its 95% confidence interval. The dashed line shows the relative susceptibility decrease using the previously published rate (g = 0.1).

Transmission parameters estimation

The environmental transmission model parameters were estimated from experimental calf-to-calf and cow-to-calf transmission data using maximum likelihood estimation. These included the decay rate estimate for *MAP* in the environment ($\widehat{de}$); transmission rate parameter estimates, which were state-specific ($\widehat{\beta_{Itr}}$, $\widehat{\beta_{Il}}$, $\widehat{\beta_{Ih}}$) in Model A, and constant ($\hat{\beta}$) in Model B; and shedding rate estimates, which were constant ($\widehat{sh}$) in Model A, and state-specific ($\widehat{sh_{Itr}}$, $\widehat{sh_{Il}}$, $\widehat{sh_{Ih}}$) in Model B. In both models, the reference infectious state is Itr, which means that the constant $\widehat{sh}$ in model A is equivalent to $\widehat{sh_{Itr}}$ in model B, and the constant $\hat{\beta}$ in model B is equivalent to $\widehat{\beta_{Itr}}$ in model A. This is defined according to the model's unit structure, as the unit

of $E_{state}(t)$ is standardized based on exposure levels. Specifically, in a clean environment, the exposure from a single infectious individual in the Itr state over one week is set to one unit, such that $\int_0^1 E_{Itr}(t) = 1$. Profile likelihood visualizations for each parameter are shown in Fig 3, with detailed results in Table 2.

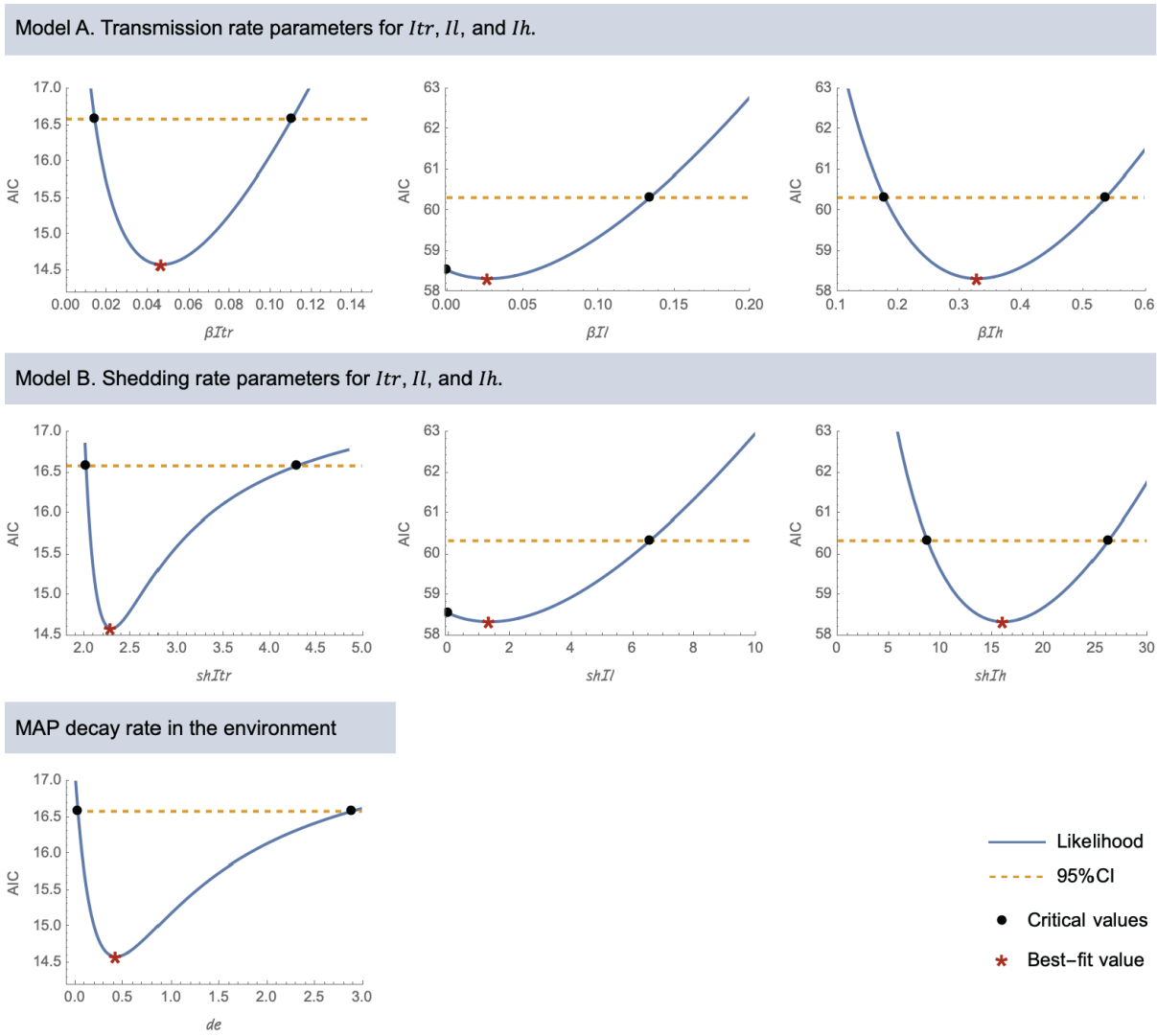

Fig 3. Profile-Likelihood Plots for Shedding, Transmission, and Decay Rate Parameters. The first row represents results from Model A, where shedding remains constant across all infectious states (is not shown, but equivalent to sh_{Itr} as Itr is the reference infectious state), with differences reflected in the transmission rate parameters (β_{Itr}, β_{Il}, β_{Ih}). The second row represents results from Model B, where

variations are reflected in shedding rate parameters (sh_{Itr}, sh_{Il}, sh_{Ih}), while transmission rate remains constant (is not shown, but equivalent to β_{Itr} as Itr is the reference infectious state). In both models, the decay of MAP in the environment (de) is independent of infectious states and remains constant. The best estimate for each parameter corresponds to the lowest AIC value, marked by a red star. The solid dots represent the critical values for the 95% confidence interval, which is defined by minimum AIC+2 (the dashed line).

Table 2. Profile Likelihood Estimates and 95% Confidence Intervals for Transmission, Shedding, and Decay Rate Parameters in Model A and B (Units: wk^{-1})

	Transmission Rate Parameter Estimates ($\hat{\beta}$)			Shedding Rate Parameter Estimates ($\widehat{sh}$)			Decay Rate Parameter Estimates ($\widehat{de}$)
	$\widehat{\beta_{Itr}}$	$\widehat{\beta_{Il}}$	$\widehat{\beta_{Ih}}$	$\widehat{sh_{Itr}}$	$\widehat{sh_{Il}}$	$\widehat{sh_{Ih}}$	
Model A	0.0469 (0.0141, 0.111)	0.0272 (0,0.134)	0.329 (0.178, 0.536)	2.29 (2.02, 4.29)			0.424 (0.0260, 2.89)
Model B	0.0469 (0.0141, 0.111)			2.29 (2.02, 4.29)	1.33 (0, 6.55)	16.1 (8.70, 26.22)	

Model fit evaluation

Model fit is assessed by comparing predicted infection probabilities with actual experimental observations. During Experiment A1, 3 high shedders and 3 low shedders were observed; during Experiment A2, 4 transient shedders were present. During Experiment B1, 1 high shedder, 3 low shedders, and 2 non-infected cows were observed, while during Experiment B2, no infectious individuals were observed. As detailed in the Materials & Methods section, in Experiments A1 and B1, 6 cows

were housed in individual pens, with 5 recipient calves placed between each pair of cows, and calves' positions were randomly switched every two weeks. For simplicity, this setup was treated as a "pairwise" experiment, where one cow and one calf are paired. As there was no specific information regarding the location of cows and calves in the experiment A1 or B1, the infectivity of the shedder in each pair was considered as the average across all 6 infected cows. In experiments A2 and B2, five shedders and five recipient calves were placed in the same pen, allowing for unrestricted contact between all animals. Based on the amount and infectious state of individuals in each experiment, the environmental contamination levels ($E_{state}(t)$), population force of infection ($\lambda tot_{0,t}$), total recipient susceptibility($RS_{0,t}$), and infection probabilities($p_{0,t}$) were calculated according to Equations 3, 6–8.

As shown in Fig 4, the curve and shaded area (left axis) represent the predicted infection probabilities over time (0, t), while the bar plot (right axis) displays the observed data from the experiments. The visualization indicates a good fit of the model, as the predictions aligns with the observed data, demonstrating that the model effectively captures the dynamics of infection transmission. Besides, the total infection probabilities over the whole experiment duration and the predicted number of infections were calculated. The predicted overall infection probabilities for experiment A1, A2, B1, B2 are 96.2%, 42.4%, 71.7%, 0.00%. As there are five recipients in each experiment, the expected number of new infections is calculated to be 4.81, 2.12, 3.58, 0.00 respectively, while 5, 2, 4, 0 infections were observed. Therefore, it can be concluded that our model has quite good model fit. Additionally, to verify the estimated $\widehat{de}$, we compare it with culture-based data on *MAP* viability in cattle excretions. For instance, in faecal pellet samples collected from partially

shaded pasture at 10-22℃, the decay rate was estimated to be 0.461 wk^{-1}. Similarly, in cattle slurry under temperatures of 5℃ and 15℃, the decay rates were 0.353 wk^{-1} and 0.908 wk^{-1}, respectively. These values provide a range for comparison with the model's predictions(7, 14, 21-27). Further details can be found in S1 File.

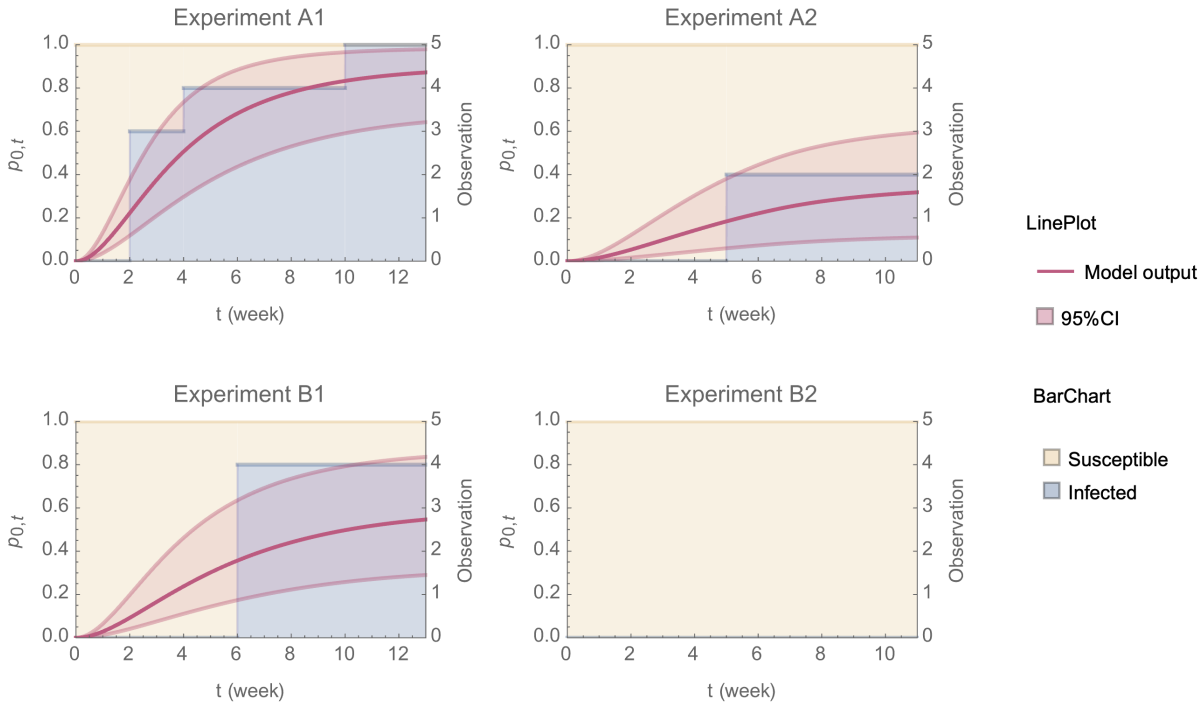

Fig 4. Comparison of Predicted Accumulative Infection Probabilities with Experimental Observations. The four plots show parallel cow-to-calf experiments (A1 & B1) and parallel calf-to-calf experiments (A2 & B2). The solid curve and shaded area represent the predicted accumulative infection probabilities their 95% confidence interval from start of experiments(t=0) to time t. The blue bars indicate the number of newly infected individuals observed in the experiments. The x-axis denotes time in weeks, with the left y-axis showing infection probability and the right y-axis showing the number of susceptible and infected individuals.

Scenario study

A scenario study was conducted to simulate changes in $E_{state}(t)$ over contamination duration and to evaluate the effects of exposure timing, duration, and the recipient's age on infection probability. Fig 5 and 6 present results of the scenario study. In Scenario 1, $E_{state}(t)$, $\lambda_{state}(t)$, and t_{eq} were calculated for environments with the presence of an infectious individual in states Itr, Il or Ih. As shown in Fig 5, environmental contamination levels rapidly increase and then stabilize at equilibrium in both model A and B. The time (teq) to reach 99% of the environmental contamination equilibrium level was calculated to be 10.8 weeks for all infectious states in both Model A and Model B. As described in 2.4, eq can be set to any time point after equilibrium, so was assumed to be 60 weeks in later analysis. Despite the difference in $E_{state}(t)$, both models result in the same $\lambda_{state}(t)$ (Fig 6, Scenario 1). At equilibrium, Ih has the highest $\lambda_{Ih}(t_{eq})$ value at 1.77 (0.959, 2.89) wk^{-1}, while Il and Itr had similar values of 0.147 (0, 0.723) wk^{-1} and 0.253 (0.076, 0.596) wk^{-1}, respectively.

Scenario 2 assessed the infection probability for exposing a fully susceptible individual to the previously defined three types of environments for 1 week, with the variable being the timing of exposure x. As shown in Fig 6-Scenario 2, the infection probabilities firstly increased and then stabilized at 21.7% (7.1% to 44.2%) for Itr, 13.3% (0% to 50.7%) for Il, and 82.1% (60.2% to 94.1%) for Ih. In Scenario 3, extending the exposure time y results in a rapid increase in infection probabilities. For Ih, the infection probability approaches 100% after approximately 3.31 weeks (to two decimal places). However, for Itr and Il, the probabilities do not reach 100% due to the decreasing susceptibility over age/time but still reach 89.4% and 97.9%

respectively by the end of 52 weeks. In Scenario 4, infection probabilities decrease with age z. By the end of calfhood (52 weeks old), the probabilities and their 95% confidence intervals are: 0.928% (0.108% to 5.56%) for Itr, 0.540% (0% to 6.70%) for Il, 6.33% (1.35% to 2.42%) for Ih.

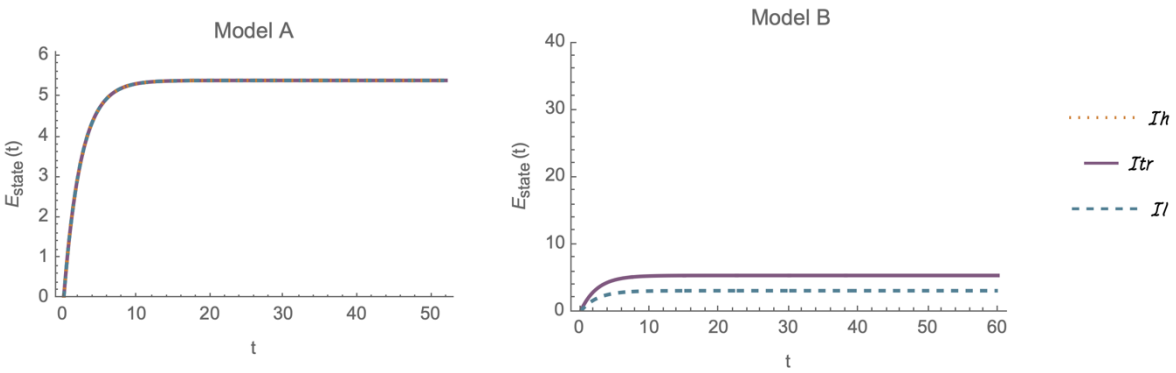

Fig 5. Changes in $E_{state}(t)$ over time while there is one Infectious individual in states Itr, Il or Ih: In Model A (left), infectious individuals in different states have the same shedding rate, while in Model B (right), $E_{state}(t)$ increases at different rates due to varying shedding rates among infectious states. The natural decay rate of MAP is constant in both models.

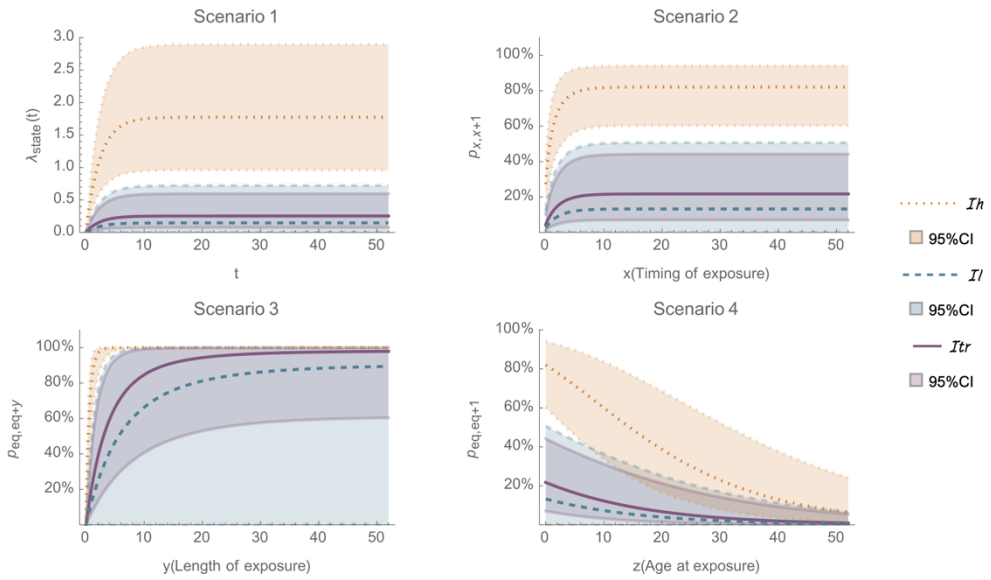

Fig 6. Results of the scenario study: (1) Changes of force of infection rate per individual ($\lambda_{state}(t)$) over time with the presence of one infectious individual at Itr, Il or Ih states; (2) Predicted infection probabilities for a fully susceptible individual exposed to the contaminated environment at time x (for x ∈[0,52]) after the start of contamination (x=0), with each exposure lasting for a 1-week interval; (3) Predicted infection probabilities for a fully susceptible individual exposed to the contaminated environment at equilibrium, across varying exposure durations y (for y ∈[0,52]); (4) Predicted probabilities of infection for susceptible individuals of age z (for z ∈[0,52]) exposed to the contaminated environment at equilibrium 1, over a 1-week exposure interval. In all four results, solid, dashed, and dotted lines represent the infectious individual at states Itr, Il, and Ih, respectively. The shaded areas represent the corresponding 95% confidence intervals, calculated based on the 95% confidence intervals of transmission rate parameters and the age-specific susceptibility decrease rate.

This research aims to improve understanding of *MAP* transmission dynamics through a novel mathematical model, which has not been previously applied to *MAP*. While comparisons with earlier studies are insightful, differences in transmission mechanism assumptions do complicate direct comparisons. However, the force of infection rates and infection probabilities can still be helpful for evaluating our findings alongside previous research. Therefore, we used a different and commonly used dose-response transmission model (19) and the parameters relevant to that model to replicate the model fit evaluation and scenario analyse. Both models fit the cow-to-calf experimental observations reasonably well; however, a significant difference is noticed in calf-to-calf transmission. The predicted number of new cases

over the entire period of experiments A1, A2, B1, and B2, based on another model constructed according to previously published model(19), were 5.00, 0.00, 3.98, and 0.00, respectively. These predictions are different in that they model that there is no calf-to-calf transmission whereas the observed values were 5, 2, 4, and 0, respectively. Detailed model descriptions, results, and discussions are provided in S2 File.

Discussion

The aims of this research were: firstly, to develop an age-specific dose-response model to study changes in recipient susceptibility over age; secondly, to construct an environmental transmission model to quantify the parameters for the transmission dynamics of *MAP*, i.e. estimate the shedding rate parameter, transmission rate parameter and *MAP* decay rate parameter. A scenario study followed, focusing on four objectives: changes in contamination levels over time, the timing of exposure, the duration of exposure, and the recipient's age. Maximum likelihood estimation was applied to achieve the best estimates, and model fit was assessed. Additional details, including a summary of original exposure data from published experiments, culture-based data on *MAP* viability in cattle excretions, and comparisons with transmission parameters from previous research, are provided in the S1 Data.

Research has suggested that calf-to-calf transmission may be underestimated (28-31). In this study, we identified that this underestimation could be partly due to the use of a rounded value of 0.1 for the age-specific susceptibility decrease rate. Based on the exposure data of fourteen experiments, we estimated a decrease rate

parameter of 0.0629 wk^{-1} (95% CI: 0.0446, 0.0811 wk^{-1}). As shown in Fig. 2, starting from a standardized average susceptibility of 1 for newborns, this value declines to 0.5 after 11 weeks and further drops to 0.0380 by 52 weeks of age. In contrast, the commonly used rate of 0.1 wk^{-1} results in susceptibility dropping to 0.5 at 6.93 weeks and to 0.00552 by 52 weeks. This suggests that if a 52-week-old calf is exposed to a stabilized contaminated environment from Ih for one week, the expected infection probability would be 0.927%, which is significantly lower than our estimate of 6.33% (with a 95% CI of 1.35% to 24.2%). Our prediction aligns more closely with observations of new infections in heifers and older calves (Mortier et al., 2013; Payne & Rankin, 1961a), and could therefore improve the evaluation of calf-to-calf transmission and inform more effective interventions.

Transmission parameters were estimated using data from cow-to-calf and calf-to-calf transmission experiments. The study applied two models—Model A and B—to capture variations across different infectious states (Itr, Il, Ih) in *MAP* transmission. In Model A, the shedding rate was standardized at 2.29 (95% CI: 2.02, 4.29) wk^{-1}, with variations attributed to transmission rate parameters: $\widehat{\beta_{Itr}}$ at 0.0469 (95% CI: 0.0141, 0.111) wk^{-1}, $\widehat{\beta_{Il}}$ at 0.0272 (95% CI: 0, 0.134) wk^{-1}, and $\widehat{\beta_{Ih}}$ at 0.329 (95% CI: 0.178, 0.536) wk^{-1}. Model B varied shedding rates across infectious states: $\widehat{sh_{Itr}}$ at 2.29 (95% CI: 2.02, 4.29) wk^{-1}, $\widehat{sh_{Il}}$ at 1.33 (95% CI: 0, 6.55) wk^{-1}, and $\widehat{sh_{Ih}}$ at 16.1 (95% CI: 8.70, 26.22) wk^{-1}, while maintaining a constant transmission rate parameter at 0.0469 (95% CI: 0.0141, 0.111) wk^{-1}. In both models, the decay rate of *MAP* in the environment was the same, which was estimated at 0.424 (95% CI: 0.0260, 2.89) wk^{-1}. As shown in S1 File, the decay rate parameter is consistent with published decay rates observed in cattle farm environments, particularly with cattle faeces.

To interpret the estimates, a scenario study was conducted. The results indicate that *MAP* accumulates quickly in the environment and takes approximately 10.8 weeks to reach 99% of its equilibrium value. At equilibrium, the highest $E_{state}(t)$ is associated with Ih, followed by Itr and Il, though the difference between the latter two is much smaller. However, Il exhibits a larger 95% CI, and more importantly, Il could pose a greater overall hazard due to its longer shedding period (32). Besides, the scenario 3 shows that the exposure duration greatly affects infection probability, assuming exposing a fully susceptible recipient in a stabilized contaminated environment, the infection probabilities reach 100% for Ih after 3.31 weeks, 89.4% for Il after 52 weeks and 97.9% for Itr after 52 weeks. The probabilities for Itr and Il didn't reach 1 because increasing exposure duration also means the recipient's age increases, leading to a decrease in relative susceptibility.

A limitation of the current study is the absence of a dedicated environmental transmission experiment—specifically, one that introduces susceptible individuals into a contaminated environment without the presence of infectious individuals. Conducting such an experiment in the future could improve the accuracy of parameter estimation. Besides, the application of the estimated parameters in real farm models is more complex than in controlled lab experiments. On farms, a larger number of infected and susceptible animals at varying states and ages are involved, alongside continuous contamination processes, limited diagnostic capabilities, and more challenging hygiene management due to larger spaces. Next, multiple interventions are widely applied, further complicating quantifying the transmission dynamics. Future research should develop a continuous-time, age-structured

compartmental stochastic model that simulates *MAP* transmission at the farm level. Although several simulation models already exist, the refined transmission parameter estimates from this research have the potential to enhance simulation accuracy and improve overall reliability. Such a model would incorporate factors like age cohorts, animal grouping and movement, farm management, environmental contamination, and real-world interventions.

Materials and Methods

Age-specific susceptibility decrease rate

Literature search was conducted focusing on *MAP* inoculation experiments performed on calves with different age groups. Data were collected from experiments that provided detailed information, including inoculation dose, bacterial strain, number of experimental animals, age at inoculation, inoculation methods, diagnostic methods, and binary results (infected/not infected) (2, 3, 33-47). The initial susceptibility of new-borns is standardized to be 1 ($rS(0)$=1) and it decreases exponentially with age at a rate of g. ID_{50} is defined as the dose at which a newborn calf, when exposed, would have a 50% probability of becoming infected. To estimate g and ID_{50}, we constructed an age-specific dose-response model to calculate relative susceptibility ($rS(age)$), based on exponential distribution (Equation 1). The maximum likelihood method is applied on a stochastic model with the number of new infections following a binomial distribution, with S trials and a dose/age dependent infection probability $p(dose, age)$ (Equation 2). In the model, g is regarded as an adjustment factor influencing ID_{50}, which implies that older individuals necessitate a

higher dose of *MAP* to attain a 50% chance of infection compared to younger individuals.

$$rS(age) = e^{-g \times age} \tag{1}$$

$$p(dose, age) = 1 - e^{-\left(rS(age) \times \frac{\ln(2)}{ID_{50}}\right) \times dose} \tag{2}$$

Besides, to calculate the infection probability over an exposure period, where the age increases simultaneously over time, the average relative susceptibility can be calculated as $\overline{rS}(age_i, age_i + \tau) = \frac{1}{\tau}\int_{age_i}^{age_i+\tau} rS(\alpha)d\alpha$. This calculation provides the mean susceptibility over the time interval $(i, i + \tau)$, accounting for how susceptibility changes as the individual ages from age_i to $age_i + \tau$.

Transmission rate parameters

MAP experimental transmission data were obtained from experiments conducted by van Roermund et al. (48), which involved 12 cows and 20 calves, and aimed to replicate real-world cow-to-calf and calf-to-calf transmission scenarios. In the initial phase of the experiment, five 1-week-old naive calves were placed between each pair of six inoculated adult cows in a row. The positions of calves were altered randomly every two weeks over the period of the three-month experiment, ensuring each calf was equally exposed to all random pairs of cows beside it. Sampling of all individuals occurred once every two weeks, using three diagnostic methods, i.e., serum ELISA, bacterial culture, and interferon-gamma tests. Cows with at least one positive result (based on faecal culture) of more than 100 colonies of *MAP* per tube

(0.16 g faeces) during the seven tests were categorized as high shedders (Ih), while those with at least one positive result or no positive result were categorized as low shedders (Il) or non-infectious, respectively. This classification was also applied throughout our modelling.

Subsequently, in the second phase of the experiment, the previously contaminated five calves (including certain number of transiently infectious calves (Itr)) were brought into contact with five new 1-week-old naive calves for a period of three months. Within the calf pen, all 10 calves had unrestricted contact with each other. Similarly, like before, the three diagnostic methods were conducted once every two weeks on each calf. The whole experiment was repeated once, i.e., again 6 cows, 5 naïve calves, and these again in contact with 5 additional calves, to verify consistency and accuracy of the findings. Regular pen cleaning was performed weekly, without additional disinfection. All calves were fed artificial milk replacer, eliminating the possibility of transmission through contaminated milk. A summary of the original data from published experiments is provided in S1 Data.

MAP transmission is modelled here using a stochastic environmental transmission model (10). According to the model assumptions, the environmental contamination level ($E_{state}(t)$) is determined by the presence and shedding rate of infectious individuals at different states (s$tate = Itr$, Il or Ih), as well as the pathogen's decay rate in the environment (Equation 3).

$$\frac{dE_{state}(t)}{dt} = sh\, I_{state,t} - de\, E_{state}(t) \qquad (3)$$

with $E_{state}(0) = 0$

By solving Equation 3, $E_{state}\ (t)$ can be expressed explicitly:

$$E_{state}\ (t+\tau) = \frac{(1-e^{-de\,\tau})}{de} sh_{state}\ I_{state,t} + e^{-de\,\tau} E_{state}(t) \tag{4}$$

As described in Section 2.1, in this experimental setup, both the infectious and susceptible populations are heterogeneous, meaning that the total force of infection rate (λtot) or the total susceptibility (RS) is the sum of each infectious or susceptible individual, respectively. And within each observed time interval (i, $i+\tau$), the number of new infections occur according to a binomial distribution with S_i trials and an infection probability of:

$$p_{i,i+\tau} = 1 - e^{-\frac{\lambda tot_{i,i+\tau} \times RS_{i,i+\tau}}{N_i}} \tag{5}$$

For shedders, the force of infection per individual in a given $state$ at time t, denoted as $\lambda_{state}(t)$, is calculated as $\beta_{state} \times E_{state}(t)$. On a population level, if individuals in the I_i compartment are indexed by m, where $m \in \{1,2 \ldots I_i\}$, then the total force of infection $\lambda tot_{i,i+\tau}$ over the time interval (i, $i+\tau$) is:

$$\lambda tot_{i,i+\tau} = \sum_{m=1}^{I_i} \left(\int_{i}^{i+\tau} \beta_{state_m} \times E_{state_m}(t)\, dt \right) \tag{6}$$

For recipients, if the susceptibility level is constant across all individuals in the S_i compartment, the total susceptibility is simply the number of susceptible individuals. However, when susceptibility varies with age, the total susceptibility $RS_{i,i+\tau}$ over the

time interval $(i,\ i+\tau)$ is the sum of susceptibilities for all individuals. Let individuals in S_i be indexed by n, where $n \in \{1,2 \ldots S_i\}$, then:

$$RS_{i,i+\tau} = \sum_{n=1}^{S_i} \overline{rS}\left(age_{n,i}, age_{n,i} + \tau\right) \tag{7}$$

To express Equation 5 by substituting Equations 6 and 7 into it, the infection probability $(p_{i,i+\tau})$ during time interval $(i,\ i+\tau)$ equals:

$$p_{i,i+\tau} = 1 - e^{-\frac{\sum_{m=1}^{I_i}\left(\int_i^{i+\tau} \beta_{state_m} \times E_{state_m}(t)dt\right) \times \sum_{n=1}^{S_i} \overline{rS}\left(age_{n,i}, age_{n,i}+\tau\right)}{N_i}} \tag{8}$$

In this research, model outputs were made weekly ($\tau = 1$ wk) to track the occurrence of new infections, while the underlying model operates in continuous time. The maximum likelihood method is used to fit the model to observed infection events, with the estimates determined at the minimal Akaike Information Criterion (AIC) value. The 95%CIs are determined by adding 2 to the minimum AIC value(49). Equations for maximum likelihood estimate $(\widehat{\mathcal{L}(\theta)})$ and AIC are listed below:

$$\widehat{\mathcal{L}(\theta)} = \max_{\theta} \prod_i \left(1 - p_{i,i+1}\right)^{case_i} \ p_{i,i+1}{}^{(S_i - case_i)} \tag{9}$$

$$AIC = 4 - 2\,log\left(\widehat{\mathcal{L}(\theta)}\right) \tag{10}$$

Due to non-identifiability of the three parameters jointly, variations in the infectiousness of individuals across different states $(Itr,\ Il,\ Ih)$ may be due to the

differences in transmission rate parameters or shedding rate parameters or a combination of these. Here, we denote model A and model B to illustrate two distinct extreme representations. In model A, shedding remains constant across all infectious states, which implies that the amount of contamination produced by individuals at different states is the same, whereas the contaminants differ in their ability to cause infection, reflected in β_{state}, for state is either Itr, Il, Ih. Conversely, in model B, the difference lies in shedding amount of *MAP* over time (sh_{state}, for state is either Itr, Il, Ih), while β remains constant. Scheme plots for compartment model A and B can be found in Figure S1.

During the process of fitting exposure data to the model, two separate estimations were conducted according to Equation 6. In the calf-to-calf transmission experiment, the unknown parameters are represented as $\theta = \{de, \beta_{Itr}\}$ in both Model A and B. Because in Model B, given the estimated value of de, the value of sh_{Itr} can be inferred as follows: $sh_{Itr} = \frac{de^2}{-1+e^{-de}+de}$ (10). In the cow-to-calf transmission experiment, as de has already been calculated in calf-to-calf experiment, the unknown parameters for model A are $\theta = \{\beta_{Il}, \beta_{Ih}\}$, while the unknown parameters for model B are $\theta = \{sh_{Il}, sh_{Ih}\}$.

The reference infectious state in both models is Itr, which can be explained by the unit definition of the model. The unit of $E_{state}(t)$ differs in scale from the dose unit (CFU for *MAP*). Instead, it is standardized such that, in a clean environment, the $Exposure$ from one infectious individual at state Itr over a week is set to one unit ($\int_0^1 E_{Itr}(t)\, dt$=1). This standardization ensures a consistent interpretation of the

transmission rate parameter and shedding rate parameter across this research and other studies with different transmission mechanism assumptions.

Model fit evaluation

Model fit is assessed by comparing the predicted infection probabilities with the actual observations from the experiments. The experiment begins at time 0, and at any subsequent time point t, $p_{0,0+t}$ can be calculated using the Equation 5. The total infection probability over the whole experiment duration and the expected number of new infections can be calculated ($E(New\ case) = S_0 \times p_{0,0+t}$). This evaluation helps determine how accurately the model reflects the true dynamics of infection transmission and provide insights into how the underlying infection process may look like in the real-world experiments.

Scenario study

In this research, a scenario study was included to show the interpretation of the estimated parameters under more lifelike conditions. The study focuses on four key objectives: (1) Duration of Contamination: examining the impact of retaining an infectious individual (at state $Itr,\ Il$ or Ih) in a clean environment, simulating changes in the contamination level over time ($E_{state}(t)$), the force of infection rate over time($\lambda_{state}(t)$) and calculating time (t_{eq}) required to reach equilibrium phase. (2) Timing of Exposure: calculating infection probabilities associated with short-term exposures before equilibrium (when $E_{state}(t)$ is increasing) and after equilibrium (when $E_{state}(t)$ has stabilized). To ensure meaningful comparisons and prevent probabilities from converging to 1, the exposure interval is set to 1 week, with the

susceptible individual's age at 0 weeks at the start of exposure. (3) Duration of Exposure: Investigating how varying exposure durations influence infection probability over time. Same as Scenario 2, the assumptions are $E_{state}(t)$ is stabilized and the recipient is fully susceptible at the start. (4) Age of the Recipient: Predicting how changes in the recipient's age, along with corresponding variations in susceptibility, affect infection probability, assuming $E_{state}(t)$ is stabilized and the exposure duration is fixed at 1 week. For both Scenario 3 & 4, the total simulated duration was based on the maximum susceptible age of 52 weeks. Table 1 provides a summary of the scenario setups, variables, variation ranges, and corresponding equations.

Table 1. Overview of Scenario Study Parameters and Objectives.

Scenario	Infectious state	Exposure starts time (Week)	Length of exposure interval (Week)	Recipient's age at start of exposure (Week)	Output
1	$Itr,\ Il$ or Ih	-	-	-	$E_{state}(t)$ and $\lambda_{state}(t)$
2	$Itr,\ Il$ or Ih	x, $x \in [0,52]$	1	0	$p_{x,x+1} = 1 - e^{-\beta_{state} \times \int_x^{x+1} E_{state}(t)dt \times \overline{rS}(0,1)}$
3	$Itr,\ Il$ or Ih	eq*	y, $y \in [0,52]$	0	$p_{eq,eq+y} = 1 - e^{-\beta_{state} \times \int_{eq}^{eq+y} E_{state}(t)dt \times \overline{rS}(0,y)}$
4	$Itr,\ Il$ or Ih	eq*	1	z, $z \in [0,52]$	$p_{eq,eq+1} = 1 - e^{-\beta_{state} \times \int_{eq}^{eq+1} E_{state}(t)dt \times \overline{rS}(z,z+1)}$

* eq can be set to any time point after $E_{state}(t)$ reaches its equilibrium (t_{eq}), which will be informed in the scenario 1.

All calculations and simulations were performed using Mathematica 14.0, with machine precision applied throughout the computations to ensure numerical accuracy. All data and code used for parameter estimation, simulation, model fitness analysis and scenario analysis are available in a Git repository at https://git.wur.nl/yuqi.gao/map_para_esti.

Reference

1. Johne H, Frothingham L. Ein eigenthuemlicher fall von tuberculose beim rind. Dtsch Z Tiermed Pathol. 1895;21:438-54.
2. Mortier RAR, Barkema HW, Bystrom JM, Illanes O, Orsel K, Wolf R, et al. Evaluation of age-dependent susceptibility in calves infected with two doses of Mycobacterium avium subspecies paratuberculosis using pathology and tissue culture. Veterinary Research. 2013;44(1):94.
3. Mortier RAR, Barkema HW, De Buck J. Susceptibility to and diagnosis of Mycobacterium avium subspecies paratuberculosis infection in dairy calves: A review. Preventive Veterinary Medicine. 2015;121(3):189-98.
4. Council NR. Diagnosis and Control of Johne's Disease. Washington, DC: The National Academies Press; 2003. p. 243.
5. Nielsen S, Ersbøll A. Age at occurrence of Mycobacterium avium subspecies paratuberculosis in naturally infected dairy cows. Journal of dairy science. 2006;89(12):4557-66.
6. Nielsen SS. Transitions in diagnostic tests used for detection of Mycobacterium avium subsp. paratuberculosis infections in cattle. Veterinary Microbiology. 2008;132(3):274-82.
7. Eppleston J, Begg DJ, Dhand NK, Watt B, Whittington RJ. Environmental Survival of Mycobacterium avium subsp. paratuberculosis in Different Climatic Zones of Eastern Australia. Applied and Environmental Microbiology. 2014;80(8):2337-42.
8. Aly SS, Thurmond MC. Evaluation of Mycobacterium avium subsp paratuberculosis infection of dairy cows attributable to infection status of the dam. Journal of the American Veterinary Medical Association. 2005;227(3):450-4.
9. Whittington RJ, Windsor PA. In utero infection of cattle with Mycobacterium avium subsp. paratuberculosis: A critical review and meta-analysis. The Veterinary Journal. 2009;179(1):60-9.
10. Chang Y, de Jong MCM. A novel method to jointly estimate transmission rate and decay rate parameters in environmental transmission models. Epidemics. 2023;42:100672.
11. Chang Y, Hartemink N, Byrne AW, Gormley E, McGrath G, Tratalos JA, et al. Inferring bovine tuberculosis transmission between cattle and badgers via the environment and risk mapping. Front Vet Sci. 2023;10:1233173.
12. Gamża AM, Hagenaars TJ, Koene MGJ, de Jong MCM. Combining a parsimonious mathematical model with infection data from tailor-made experiments to understand environmental transmission. Scientific Reports. 2023;13(1):12986.
13. Gao Y, Boklund AE, Nielsen LH, Alban L, de Jong MCM. Estimating the impact of low temperature on African swine fever virus transmission through contaminated environments. Preventive Veterinary Medicine. 2023;219:105991.
14. Larsen AB, Merkal RS, Cutlip RC. Age of cattle as related to resistance to infection with Mycobacterium paratuberculosis. Am J Vet Res. 1975;36(3):255-7.
15. Hagan W. Age as a Factor in Susceptibility to Johne’s Disease. 34–40 p.
16. Windsor PA, Whittington RJ. Evidence for age susceptibility of cattle to Johne’s disease. The Veterinary Journal. 2010;184(1):37-44.

17. Rankin JD. The experimental infection of cattle with Mycobacterium johnei. IV. Adult cattle maintained in an infectious environment. J Comp Pathol. 1962;72:113-7.
18. Doyle T. Susceptibility to Johne's disease in relation to age. Vet Rec. 1953;65:363-5.
19. Marcé C, Ezanno P, Seegers H, Pfeiffer DU, Fourichon C. Predicting fadeout versus persistence of paratuberculosis in a dairy cattle herd for management and control purposes: a modelling study. Veterinary Research. 2011;42(1):36.
20. Biemans F, Tratalos J, Arnoux S, Ramsbottom G, More SJ, Ezanno P. Modelling transmission of Mycobacterium avium subspecies paratuberculosis between Irish dairy cattle herds. Veterinary Research. 2022;53(1):45.
21. Olsen JE, Jørgensen JB, Nansen P. On the reduction of Mycobacterium paratuberculosis in bovine slurry subjected to batch mesophilic or thermophilic anaerobic digestion. Agricultural Wastes. 1985;13(4):273-80.
22. EAMENS G, SPENCE S, TURNER M. Survival of Mycobacterium avium subsp paratuberculosis in amitraz cattle dip fluid. Australian Veterinary Journal. 2001;79(10):703-6.
23. Collins CH, Grange JM, Yates MD. Mycobacteria in water. Journal of Applied Bacteriology. 1984;57(2):193-211.
24. Hanifian S. Behavior of Mycobacterium avium paratuberculosis in Lighvan cheese tracked by propidium monoazide qPCR and culture. LWT. 2020;133:109886.
25. Klanicova B, Slana I, Roubal P, Pavlik I, Kralik P. Mycobacterium avium subsp. paratuberculosis survival during fermentation of soured milk products detected by culture and quantitative real time PCR methods. International Journal of Food Microbiology. 2012;157(2):150-5.
26. Whittington RJ, Marshall DJ, Nicholls PJ, Marsh IB, Reddacliff LA. Survival and dormancy of Mycobacterium avium subsp. paratuberculosis in the environment. Appl Environ Microbiol. 2004;70(5):2989-3004.
27. Jorgensen JB. Survival of Mycobacterium paratuberculosis in slurry. Nord Vet Med. 1977;29(6):267-70.
28. Corbett CS, de Jong MCM, Orsel K, De Buck J, Barkema HW. Quantifying transmission of Mycobacterium avium subsp. paratuberculosis among group-housed dairy calves. Veterinary Research. 2019;50(1):60.
29. Nigsch A, Robbe-Austerman S, Stuber TP, Paulina DPB, Gröhn YT, Schukken YH. Who infects whom?—Reconstructing infection chains of Mycobacterium avium ssp. paratuberculosis in an endemically infected dairy herd by use of genomic data. PLoS One. 2021;16(5).
30. Vass-Bognár B, Bakony M, Baumgartner W, Khol JL, Jurkovich V. Association between calf rearing technology and farm-level paratuberculosis infection in Hungarian dairy farms. Preventive Veterinary Medicine. 2022;207.
31. Weber MF, Kelton D, Eisenberg SWF, Donat K. Progress in Paratuberculosis Control Programmes for Dairy Herds. Animals. 2024;14(7):1127.
32. Mitchell RM, Whitlock RH, Gröhn YT, Schukken YH. Back to the real world: Connecting models with data. Preventive Veterinary Medicine. 2015;118(2):215-25.
33. Sweeney RW, Whitlock RH, Hamir AN, Rosenberger AE, Herr SA. Isolation of Mycobacterium paratuberculosis after oral inoculation in uninfected cattle. Am J Vet Res. 1992;53(8):1312-4.
34. Payne JM, Rankin JD. A Comparison of the Pathogenesis of Experimental Johne's Disease in Calves and Cows. Research in Veterinary Science. 1961;2(2):175-9.

35. Payne JM, Rankin JD. The Pathogenesis of Experimental Johne's Disease in Calves. Research in Veterinary Science. 1961;2(2):167-76.
36. Rankin JD. The Experimental Infection of Cattle with Mycobacterium Johnei: I. Calves Inoculated Intravenously. Journal of Comparative Pathology and Therapeutics. 1958;68:331-IN24.
37. Rankin JD. The Experimental Infection of Cattle With Mycobacterium Johnei: II. Adult Cattle Inoculated Intravenously. Journal of Comparative Pathology and Therapeutics. 1961;71:6-IN1.
38. Stuart P. Vaccination Against Johne's Disease in Cattle Exposed to Experimental Infection. British Veterinary Journal. 1965;121(7):289-318.
39. Gilmour NJL, Nisbet DI, Brotherston JG. Experimental oral infection of calves with Mycobacterium johnei. Journal of Comparative Pathology. 1965;75(3):281-6.
40. Gilmour NJL, Angus KW. The specificity and sensitivity of the fluorescent antibody test in cattle experimentally infected with Mycobacterium avium and Mycobacterium johnei. Research in Veterinary Science. 1976;20(1):6-9.
41. Johnson D, Muscoplat CC, Larsen A, Thoen C. Skin testing, fecal culture, and lymphocyte immunostimulation in cattle inoculated with Mycobacterium paratuberculosis. Am J Vet Res. 1977;38(12):2023-5.
42. Lepper A, Wilks C, Kotiw M, Whitehead J, Swart K. Sequential bacteriological observations in relation to cell-mediated and humoral antibody responses of cattle infected with Mycobacterium paratuberculosis and maintained on normal or high iron intake. Australian veterinary journal. 1989;66(2):50-5.
43. Uzonna JE, Chilton P, Whitlock RH, Habecker PL, Scott P, Sweeney RW. Efficacy of commercial and field-strain Mycobacterium paratuberculosis vaccinations with recombinant IL-12 in a bovine experimental infection model. Vaccine. 2003;21(23):3101-9.
44. Waters WR, Miller JM, Palmer MV, Stabel JR, Jones DE, Koistinen KA, et al. Early Induction of Humoral and Cellular Immune Responses during Experimental Mycobacterium avium subsp. paratuberculosis Infection of Calves. Infection and Immunity. 2003;71(9):5130-8.
45. Stabel J, Palmer M, Whitlock R. Immune responses after oral inoculation of weanling bison or beef calves with a bison or cattle isolate of Mycobacterium avium subsp. paratuberculosis. Journal of wildlife diseases. 2003;39(3):545-55.
46. Sweeney RW, Whitlock RH, McAdams S, Fyock T. Longitudinal Study of ELISA Seroreactivity to Mycobacterium Avium subsp. Paratuberculosis in Infected Cattle and Culture-Negative Herd Mates. Journal of Veterinary Diagnostic Investigation. 2006;18(1):2-6.
47. Stewart DJ, Vaughan JA, Stiles PL, Noske PJ, Tizard MLV, Prowse SJ, et al. A long-term bacteriological and immunological study in Holstein-Friesian cattle experimentally infected with Mycobacterium avium subsp. paratuberculosis and necropsy culture results for Holstein-Friesian cattle, Merino sheep and Angora goats. Veterinary Microbiology. 2007;122(1):83-96.
48. van Roermund HJW, Bakker D, Willemsen PTJ, de Jong MCM. Horizontal transmission of Mycobacterium avium subsp. paratuberculosis in cattle in an experimental setting: Calves can transmit the infection to other calves. Veterinary Microbiology. 2007;122(3):270-9.
49. Burnham K, Anderson. Information and Likelihood Theory: A Basis for Model Selection and Inference. In: Burnham KP, Anderson DR, editors. Model Selection and Multimodel Inference: A Practical Information-Theoretic Approach. New York, NY: Springer New York; 2002. p. 49-97.

Supporting information

S1 Data. Collected experimental data from previous research.

S1 Figure. Scheme of Compartmental Model in Model A and Model B. Both models include six compartments: susceptible individuals ($S_a(t)$), transiently infectious ($Itr_a(t)$), latently infected ($L_a(t)$), low-shedding infectious ($Il_a(t)$), high-shedding infectious ($Ih_a(t)$), and resistant individuals ($R_a(t)$), all indexed by age a at time t. The environmental compartment differs between the models: in Model A, all infectious states shed at the same rate (sh) but generate distinct environments ($E_{Itr}(t)$, $E_{Il}(t)$, $E_{Ih}(t)$) with varying transmission rates (β_{Itr}, β_{Il}, β_{Ih}), while in Model B, shedding rates differ by infectious state (sh_{Itr}, sh_{Il}, sh_{Ih}), with a constant transmission rate (β). The diagram shows solid arrows for transitions between individual states (though not simulated in the 3-month study), dashed arrows for *MAP* shedding and decay in the environment, and dotted arrows representing the exposure of susceptible calves. The force of infection rate ($\lambda_a(t)$) is the key component.

S1 File. Validation of estimated decay rate parameter using culture-based experimental data on *MAP* viability in cattle excretions.

S2 File. A Comparative Analysis with A Previously Published Transmission Model

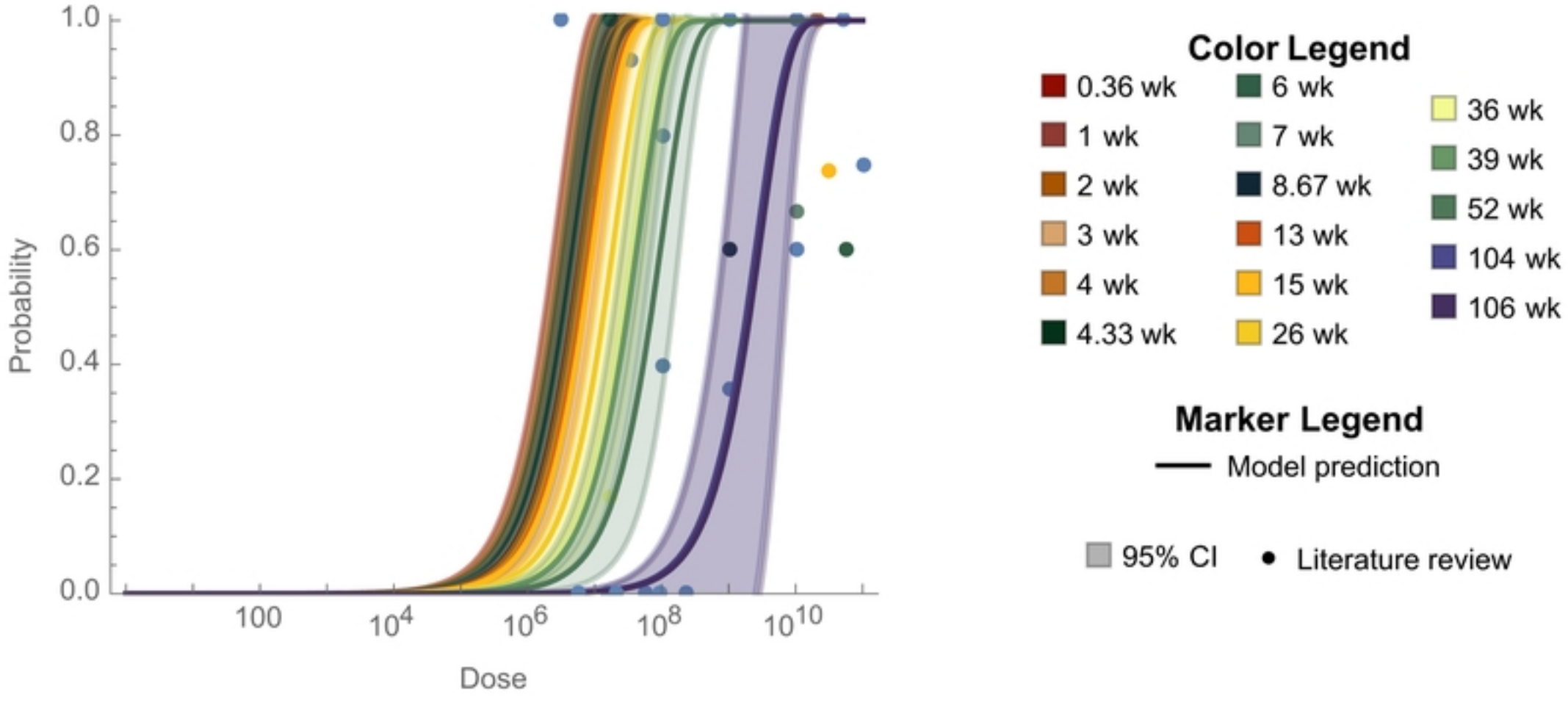
1.0
0.8
0.6
0.4
0.2
0.0
Probability
100
10^4
10^6
10^8
10^{10}
Dose
Color Legend
0.36 wk
1 wk
2 wk
3 wk
4 wk
4.33 wk
6 wk
7 wk
8.67 wk
13 wk
15 wk
26 wk
36 wk
39 wk
52 wk
104 wk
106 wk
Marker Legend
Model prediction
95% CI
Literature review

Figure

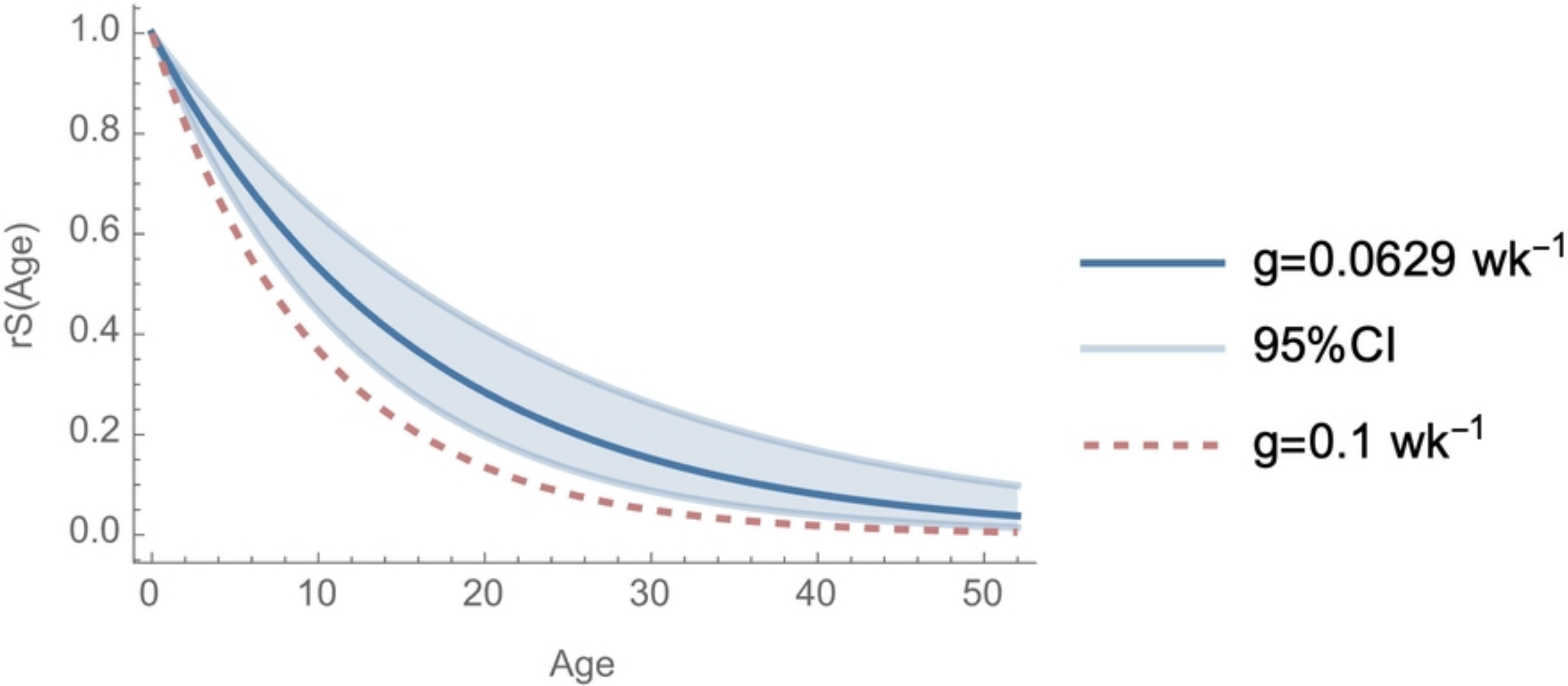
1.0
0.8
0.6
0.4
0.2
0.0
rS(Age)
0
10
20
30
40
50
Age
g=0.0629 wk^{-1}
95%CI
g=0.1 wk^{-1}

Figure

Model A. Transmission rate parameters for Itr, Il, and Ih.

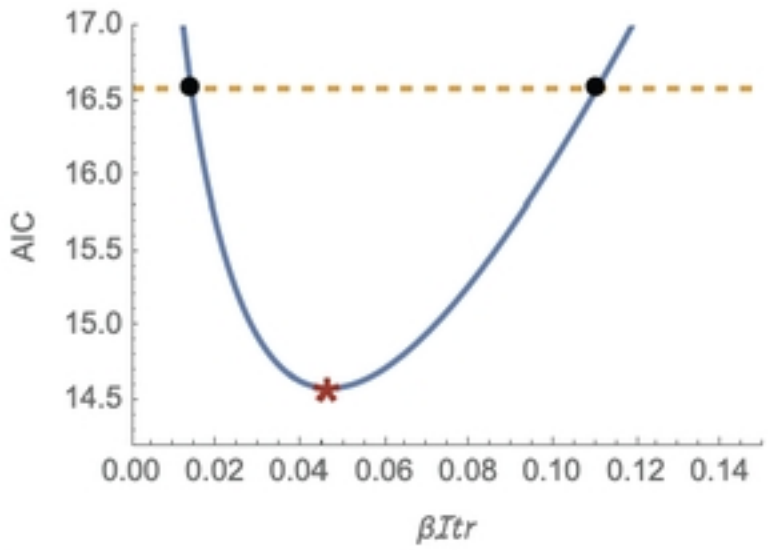

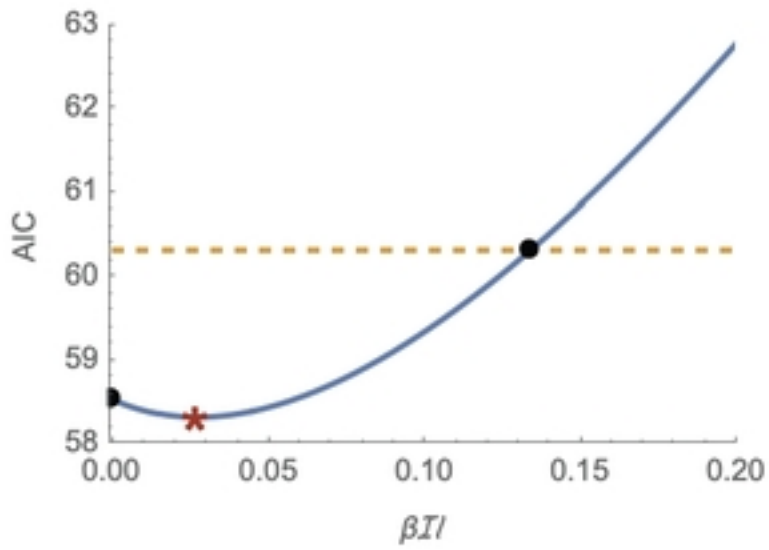

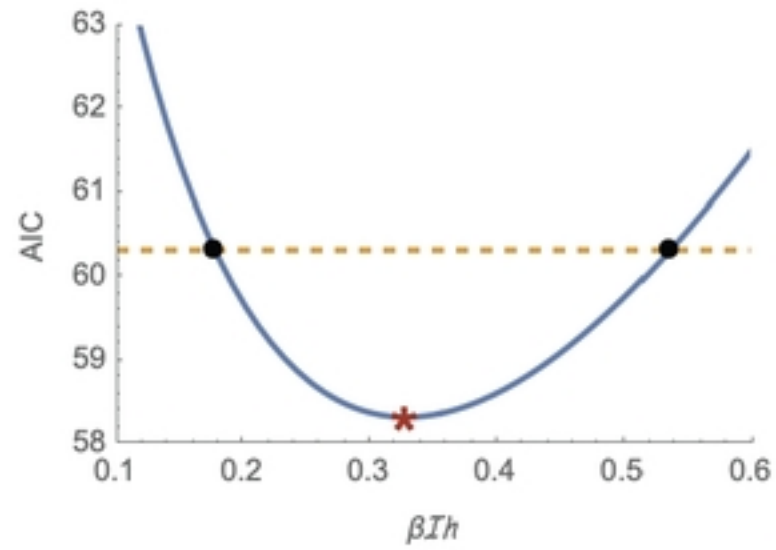

Model B. Shedding rate parameters for Itr, Il, and Ih.

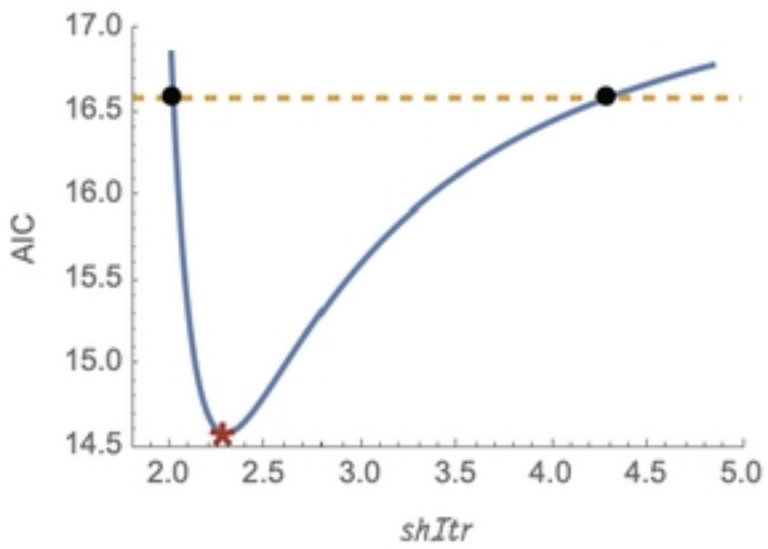

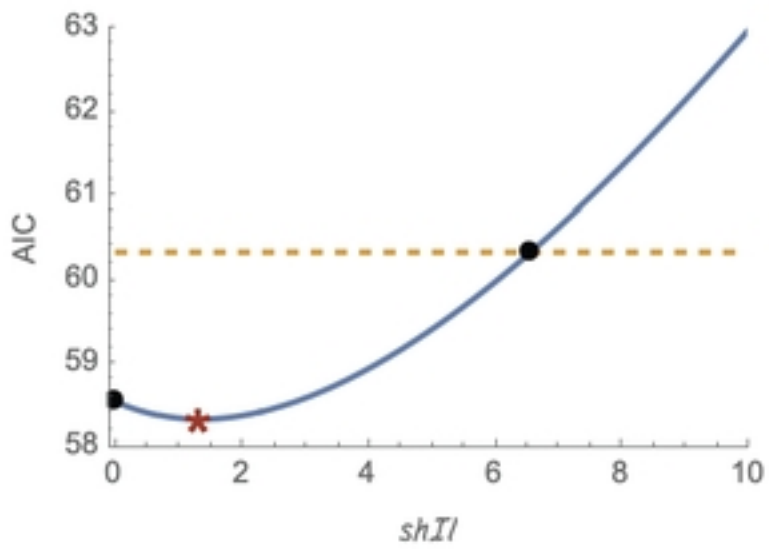

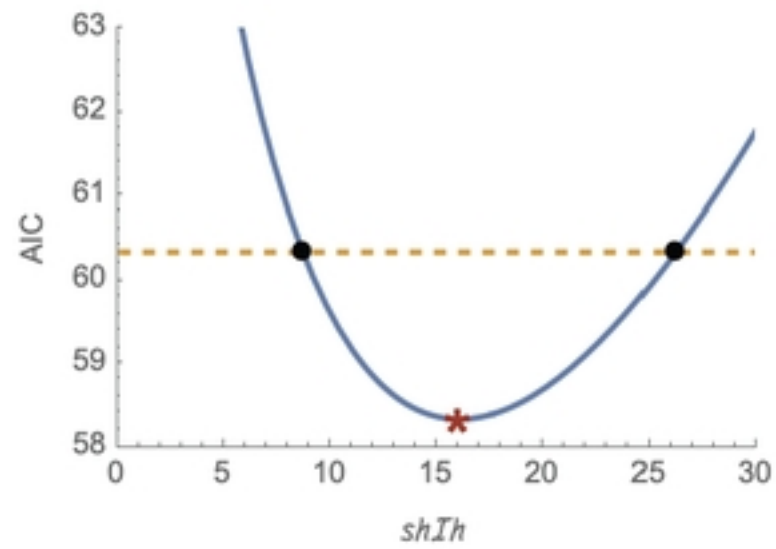

MAP decay rate in the environment

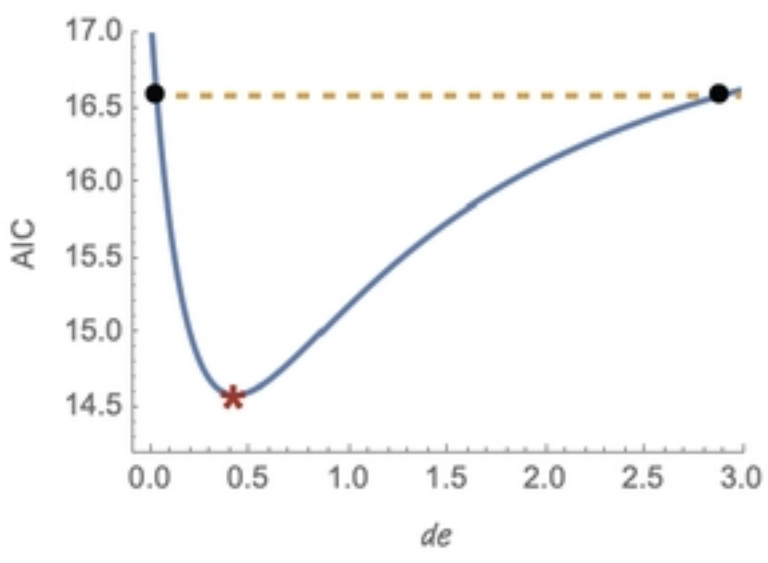

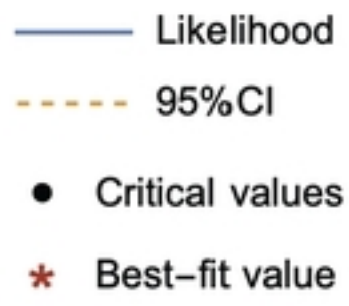

Figure

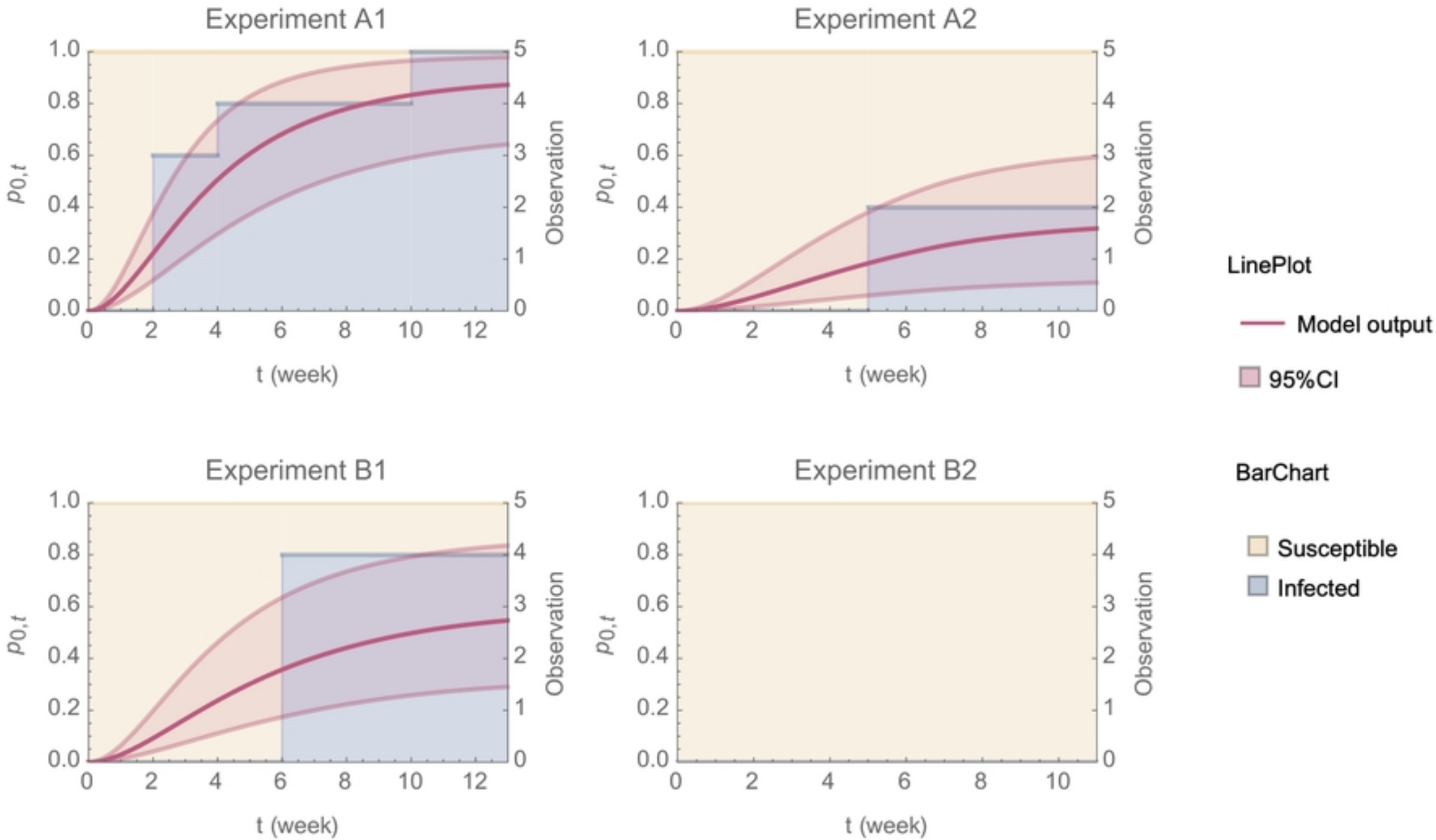
Experiment A1
Experiment A2
Experiment B1
Experiment B2
$p_{0,t}$
Observation
t (week)
LinePlot
Model output
95%CI
BarChart
Susceptible
Infected

Figure

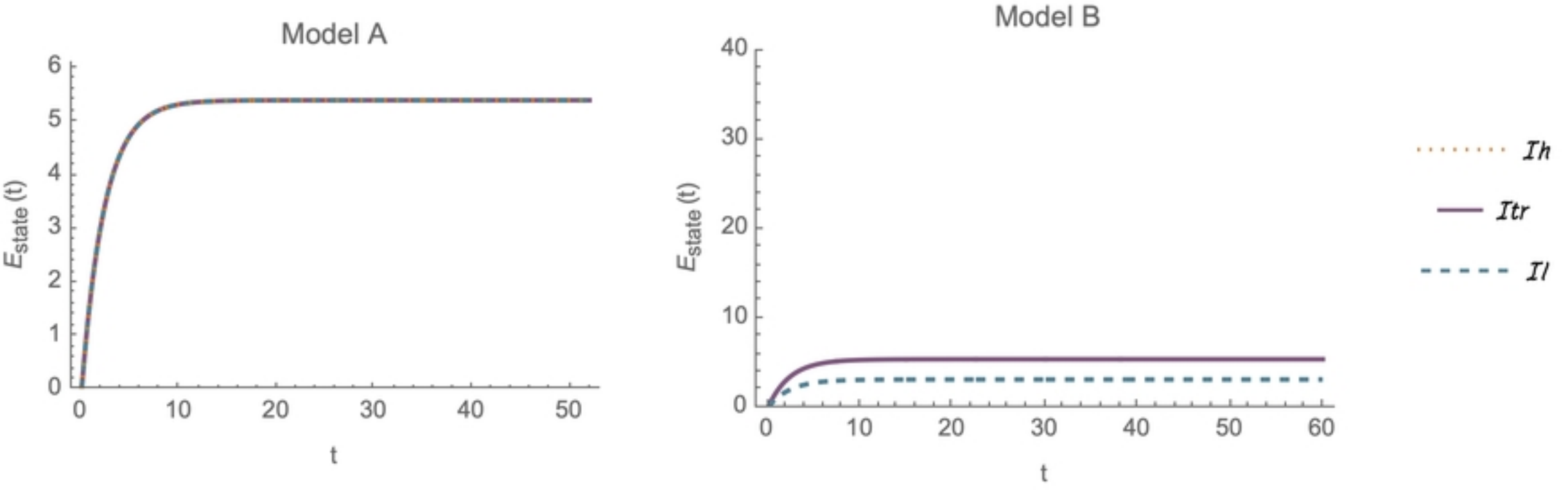

Figure

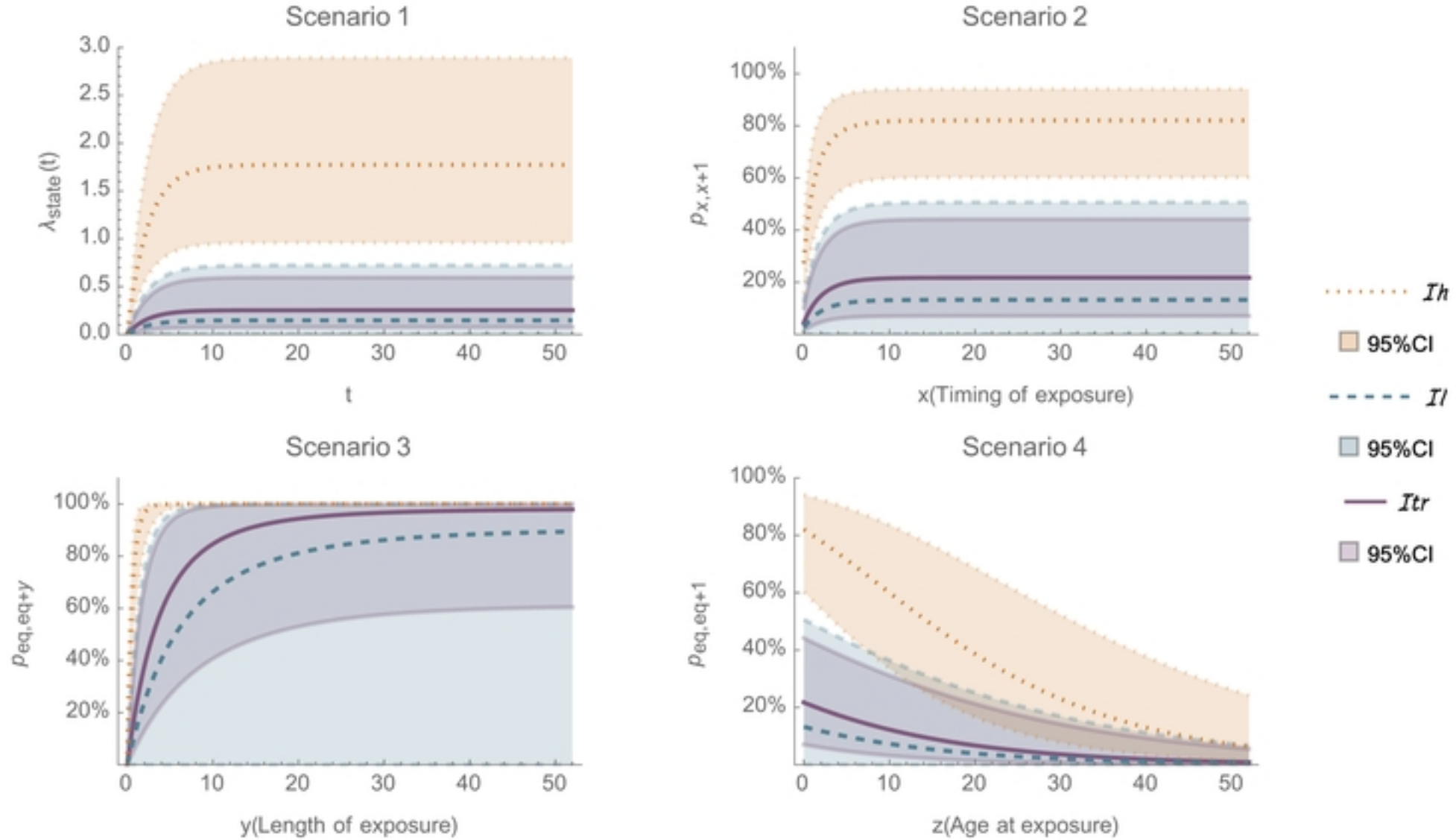
Scenario 1
λ_{state} (t)
t
Scenario 2
$p_{x,x+1}$
x(Timing of exposure)
Scenario 3
$p_{eq,eq+y}$
y(Length of exposure)
Scenario 4
$p_{eq,eq+1}$
z(Age at exposure)
Ih
95%CI
Il
95%CI
Itr
95%CI

Figure